ELSEVIER

Carbohydrate Research 267 (1995) 79–104

CARBOHYDRATE RESEARCH

Eleven newly characterized xyloglucan oligoglycosyl alditols: the specific effects of sidechain structure and location on ^{1}H NMR chemical shifts

William S. York *, Giuseppe Impallomeni [1], Makoto Hisamatsu [2], Peter Albersheim, Alan G. Darvill

Complex Carbohydrate Research Center and Department of Biochemistry and Molecular Biology, The University of Georgia, 220 Riverbend Road, Athens, GA 30602, USA

Received 25 April 1994; accepted 8 August 1994

Abstract

Eleven previously uncharacterized oligosaccharides, each containing from seventeen to twenty glycosyl residues, were isolated from the xyloglucan produced by suspension-cultured *Acer pseudoplatanus* cells and characterized by ^{1}H NMR spectroscopy, fast-atom bombardment mass spectrometry, and matrix-assisted laser-desorption mass spectrometry. The complex mixture of xyloglucan oligosaccharides released by *endo*-(1→4)-β-glucanase (*Trichoderma reesei*) treatment of cell walls was similar to that released by digestion of the soluble xyloglucan present in the culture medium. The oligosaccharides were converted to oligoglycosyl alditols by borohydride reduction and purified by a combination of gel-permeation (Bio-Gel P-2) chromatography, normal-phase HPLC, reversed-phase HPLC, and high-performance anion-exchange (HPAE) chromatography. Eleven new oligoglycosyl alditols (along with several others that had been previously characterized) were isolated and characterized, allowing additional correlations between xyloglucan structure and specific chemical shift effects in the ^{1}H NMR spectra to be determined. The correlations between structural and spectral features deduced in this study will facilitate the structural determination of a wide range of xyloglucans and their subunit oligosaccharides.

Keywords: Xyloglucan; Oligosaccharide; Structure; ^{1}H NMR spectroscopy; ^{1}H NMR chemical shifts

* Corresponding author.

[1] Present address: Consiglio Nazionale delle Richerche, Istituto per la Chimica e la Tecnologia dei Materiali Polimerici, Viale A. Doria 6, 95125 Catania, Italy.

[2] Present address: Faculty of Bioresources, Mie University, 1515 Kamihama, Tsu 514, Japan.

SSDI 0008-6215(94)00287-8

1. Introduction

Xyloglucans (XGs) are considered to be major load-bearing structures in the primary cell walls of higher plants due to their ability to noncovalently cross-link cellulose microfibrils [1]. It has been suggested that the rate of primary cell-wall expansion during cell growth is determined in part by the rate at which xyloglucan is metabolized by *endo*-(1→4)-β-D-glucanases (EGs) and *endo*-transglycanases in the cell wall [2–4]. The substrate specificity of these endogenous plant enzymes is similar to those of the fungal EG used in this study in that all of these enzymes attack unbranched β-D-Glc*p* residues in the XG backbone. However, the effects of the sidechain substitution pattern on the susceptibility of XG substrates to hydrolysis by the plant enzymes have not been studied thoroughly, due to the lack of well-defined, pure substrates and the difficulty of isolating and fully characterizing reaction products that contain over ten glycosyl residues. We report herein improved techniques for separating and structurally characterizing XG oligosaccharides with unbranched glucosyl residues in the backbone. These techniques will facilitate the thorough characterization of XG-metabolizing enzymes found in plant cell walls.

Xyloglucans (XGs) consist of a cellulosic backbone in which up to 75% of the β-(1→4)-linked D-Glc*p* residues are substituted at O-6 with α-D-Xyl*p* residues [1,5,6]. The α-D-Xyl*p* residues are frequently substituted at O-2 with β-D-Gal*p* residues or α-L-Fuc*p*-(1→2)-β-D-Gal*p* moieties. The β-D-Gal*p* residue in some XGs have *O*-acetyl substituents, predominantly at O-6 [7,8]. β-D-Xyl*p* residues are attached to O-2 of less than 5% of the β-D-Glc*p* residues in the backbone of the soluble XG secreted by suspension-cultured sycamore (*Acer psuedoplatanus*) cells [9]. Approximately 2% of this XG consists of terminal α-L-Ara*f* residues that are either attached directly to O-2 of β-D-Glc*p* residues in the backbone or to O-3 of intervening β-D-Xyl*p* residues [9].

The unbranched (1→4)-linked β-D-Glc*p* residues of XGs are normally susceptible to hydrolysis by fungal EGs. However, certain patterns of sidechain substitution reduce the susceptibility of adjacent unbranched β-D-Glc*p* residues to EG-catalyzed hydrolysis. Several large ($dp \geq 17$) oligosaccharides with EG-resistant unbranched β-D-Glc*p* residues have been isolated from the soluble XG secreted by cultured sycamore cells [9]. The resistance to EG-catalyzed hydrolysis exhibited by some of these oligosaccharides is due to the presence of an α-L-Ara*f* and/or β-D-Xyl*p* containing sidechain at O-2 of the backbone residue adjacent to the unbranched β-D-Glc*p* residue [9]. In addition, the presence of several terminal β-D-Gal*p* residues and/or α-L-Fuc*p*-(1→2)-β-D-Gal*p* moieties at O-2 of α-D-Xyl*p* residues in nearby sidechains decreases, but does not abolish, the susceptibility of the unbranched β-D-Glc*p* residues to hydrolysis by the EG [9,10]. The profound effects of sidechain substitution patterns on the location and rate of EG-catalyzed hydrolysis of XGs suggests that similar effects may play an important role in controlling XG metabolism in vivo.

The XG deposited in the cell walls of suspension-cultured sycamore cells is more difficult to structurally characterize than the soluble secreted form. Solubilization of the cell-wall bound form requires either strongly alkaline conditions or the use of EGs that hydrolyze some of the glucosidic linkages in the backbone. However, the structures of many of the smaller ($dp \leq 11$) oligosaccharides released from the cell wall by EG have been determined [5,8] and found to be identical to those released from the the soluble XG. The analysis of

the large, EG-resistant XG oligosaccharides released from the cell walls of suspension-cultured cells by EG are described herein. This analysis indicates that the structural features that were shown [9] to confer EG resistance to unbranched β-D-Glc*p* residues in the soluble XG are also present (in approximately the same proportion) in the cell-wall bound XG. Thus, XGs and XG oligosaccharides obtained from the culture filtrate of suspension-cultured sycamore cells provide a convenient source of physiologically relevant substrates for the analysis of enzymes that metabolize XG in the growing cell wall.

Spectroscopic analysis of the oligosaccharides described herein provided the basis for establishing additional correlations between specific substructures in borohydride-reduced XG oligosaccharides (i.e., oligoglycosyl alditols) and the chemical shifts of diagnostic resonances in their ^{1}H NMR spectra. These correlations provide information regarding both the identity and location of various sidechains in the oligoglycosyl alditols, and thus make it possible to rapidly and accurately determine the structures of XG fragments released by fungal or plant enzymes. This, in turn, will facilitate studies of xyloglucan metabolism in vivo and thereby enhance our understanding of the processes that contribute to the development of the primary cell wall of higher plants.

2. Materials and methods

Isolation of oligoglycosyl alditols.—Soluble XG was isolated as previously described [11] from the mixture of polysaccharides secreted by suspension-cultured XG sycamore (*Acer pseudoplatanus*) cells, commonly referred to as Sycamore Extracellular Poly-Saccharides (SEPS). The procedure used to isolate SEPS XG includes a treatment with aqueous alkali that hydolyzes the *O*-acetyl substituents present in the native polysaccharide.

Oligosaccharides (604 mg) were generated [9] from SEPS XG (620 mg) by treatment with EG [i.e., *endo*-(1→4)-β-D-glucanase, EC 3.2.1.4] purified [5] from cultures of the cellulolytic fungus *Trichoderma reesei*. In addition, oligosaccharide fragments of cell-wall bound XG [5] (CW XG) were generated by two EG treatments (each with 12 units of EG in 10 mM NaOAc, pH 5.2, for 12 h at 40°C) of purified sycamore cell walls (12.0 g) which had been previously extracted [11] with an *endo*-(1→4)-α-D-polygalacturonase (EC 3.2.1.15) isolated [12] from a commercial preparation of pectin-degrading enzymes. The acidic components of the material released from the cell walls by EG were removed by adjusting the pH of the extract to 7.0 with NaOH and passing the solution through a column of DEAE Sephadex (3.5×32 cm, Sigma) that had been equilibrated with 10 mM imidazole·HCl, pH 7.0. The neutral material (415 mg) eluted from the DEAE Sephadex column corresponds to fraction "C-1" described by Bauer et al. [5], and is composed predominantly of XG oligosaccharides. This fraction was desalted by chromatography on Sephadex G-10, yielding 405 mg of CW XG oligosaccharides.

Oligosaccharides generated from SEPS XG and CW XG were fractionated according to molecular weight by Bio-Gel P-2 chromatography. Oligosaccharides with dp's of 17–20 were eluted from Bio-Gel P-2 as a broad peak ($K_{av}=0.11$) [9]. *O*-Acetyl substituents [7] were removed from the cell-wall derived dp 17–20 oligosaccharides (49 mg) by hydrolysis in alkali (0.1 M NaOH, 1 h, 24°C). The saponified products were neutralized and desalted on Sephadex G-10 (Sigma). Conversely, the dp 17–20 oligosaccharides (102 mg) obtained

from SEPS XG were not treated with base, as the SEPS XG had been *O*-deacetylated prior to EG treatment. The dp 17–20 oligosaccharides from both SEPS XG and CW XG were fractionated by normal-phase HPLC on an amino-bonded silica gel column (Dynamax-60A, 0.6×27 cm, Rainin) eluted with either 54% (SEPS) or 62% (CW) aq MeCN, as previously described [9] (see Fig. 2). The total amount of oligosaccharide recovered was estimated colorimetrically as follows: 4.2 mg of (SEPS) N1, 31.8 mg of (SEPS) N2, 32.4 mg of (SEPS) N3, 14.4 mg of (SEPS) N4, 5.2 mg of (CW) N5, 12.1 mg of (CW) N6, 13.4 mg of (CW) N7, and 8.6 mg of (CW) N8.

The partially purified XG oligosaccharides were converted to the corresponding oligoglycosyl alditols with $NaBH_4$ (10 mg/mL in 1 M NH_4OH, 24°C). After 1 h, the pH of the mixture was adjusted to ~5.5, and the oligoglycosyl alditols were desalted on either Sephadex G-10 or G-15. The desalted oligoglycosyl alditols were further fractionated by reversed-phase chromatography on octadecylsilyl silica gel columns (Hibar Lichrosorb RP-18, 0.25×25 cm analytical and 1.0×25 cm semipreparative) eluted with aq MeOH (see Fig. 3 for details). Some of the fractions obtained by reversed-phase HPLC were further purified by high-pH anion-exchange (HPAE) chromatography with pulsed amperometric detection on a Dionex CarboPac PA1 column (4×250 mm) eluted with a linear gradient (60→150 mM NaOAc in 100 mM NaOH, 40 min total time) at a flow rate of 1.0 mL/min.

Matrix-assisted laser-desorption time of flight spectrometry (MALD-TOF).—Aqueous solutions (5 μL, ~1 μg/μL) of oligoglycosyl alditols were mixed with an equal volume of 100 mM 2,4-dihydroxybenzoic acid in 90% aq MeOH. Approximately 1 μL of this mixture was applied to the MALD probe and dried under vaccuum. MALD-TOF spectra were recorded with a Hewlett–Packard (LDI 1700 XP) TOF spectrometer operating at 30 kV accelerating voltage and a pressure of 0.4×10^{-6} to 1.1×10^{-6} torr. Ion desorption was accomplished with a nitrogen laser ($\lambda=337$ nm) with a pulse width of 3 ns and an average laser energy of ~7 μJ per pulse.

FAB-mass spectrometry.—FAB-mass spectra were recorded with a VG Analytical ZAB-SE mass spectrometer operating at low resolution (1:1000) with an accelerating voltage of 8 kV. Underivatized oligoglycosyl alditols (1 μL of a ~10 μg/μL solution in H_2O) were mixed on the probe tip with 3-amino-1,2-propanediol (2 μL, Aldrich) for negative-ion FABMS. In addition, oligoglycosyl alditols (100 μg) were *O*-peracetylated [13] with a mixture of trifluoroacetic anhydride and AcOH for positive-ion FABMS. Each *O*-peracetylated oligoglycosyl alditol (1 μL of a 10 μg/μL solution in MeOH) was mixed on the probe tip with 1-thioglycerol (3-mercapto-1,2-propanediol, 2 μL, Aldrich). The nominal masses reported herein were calculated from the observed monoisotopic exact masses of resolved isotopomers or from the chemical masses of unresolved high-mass ion clusters using the CARBOMASS [14] software developed in this laboratory.

NMR spectroscopy.—Hydroxyl protons of the oligoglycosyl alditols (0.5–5 mg) were exchanged with deuterons, samples were dissolved in D_2O (0.5 mL), and NMR spectra were recorded at ~299 K (HDO line at δ 4.75 ± 0.01 relative to internal acetone at δ 2.225) with a Bruker AM 500 NMR spectrometer. Double-quantum filtered {^{1}H,^{1}H} COSY [15] spectra and 2D ^{1}H TOCSY [16] (HOHAHA) spectra were obtained under previously described [6] conditions. Proton pulses for the TOCSY experiments were generated by the decoupler.

Table 1
One-letter codes for differently substituted β-D-Glc*p* residues in xyloglucan oligosaccharides

Structure represented	Code letter	Mnemonic
-β-D-Glc*p*-	G	Glucose
-β-D-Glc*p*- α-D-Xyl*p*-(1→6)┘	X	Xylose
-β-D-Glc*p*- β-D-Gal*p*-(1→2)-α-D-Xyl*p*-(1→6)┘	L	gaLactose
-β-D-Glc*p*- α-L-Fuc*p*-(1→2)-β-D-Gal*p*-(1→2)-α-D-Xyl*p*-(1→6)┘	F	Fucose
α-L-Ara*f*-(1→2)┐ -β-D-Glc*p*- α-D-Xyl*p*-(1→6)┘	A	Arabinose
β-D-Xyl*p*-(1→2)┐ -β-D-Glc*p*- α-D-Xyl*p*-(1→6)┘	B	Beta-xylose
α-L-Ara*f*-(1→3)-β-D-Xyl*p*-(1→2)┐ -β-D-Glc*p*- α-D-Xyl*p*-(1→6)┘	C	Follows A and B

Conformational energy calculations.—The three-dimensional conformations of the XG oligosaccharides were simulated using the GEometry of GlycOProteins (GEGOP) program [17] and visualized with the SYBYL molecular modeling software (Tripos Associates, St. Louis, MO).

Nomenclature for XG oligoglycosyl alditols.—The sequences of xyloglucan oligosaccharides are expressed as series of uppercase letters each of which represent the branching pattern of an individual β-D-Glc*p* residues in the backbone (see [18] and Table 1). Each code letter represents the entire substructure, including both the sidechain(s) and the backbone β-D-Glc*p* residue itself. For example, the letter "G" represents a β-D-Glc*p* or reducing D-Glc residue with no sidechains attached, and the letter "X" represents a β-D-Glc*p* residue with a terminal α-D-Xyl*p* residue attached at O-6. The structure of a xyloglucan oligosaccharide is thus written by starting at the nonreducing end and sequentially listing, from left to right, the code letters that represent the patterns of sidechain substitution for the

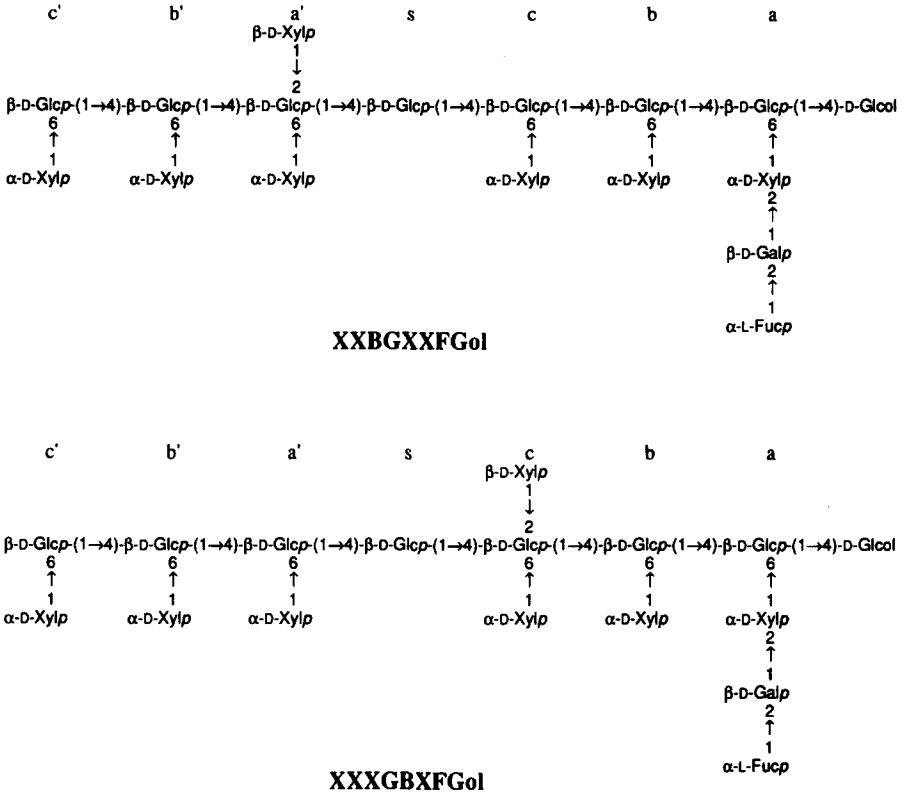

Fig. 1. Structures of the eleven newly characterized XG oligoglycosyl alditols. Abbreviations for each oligoglycosyl alditol are given by the nomenclature defined in Table 1. The lower-case letters (a, b, c, s, a′, b′, and c′) are used as superscripts to indicate the locations of specific residues within these oligoglycosyl alditols. For example, Glc^a is attached directly to the alditol moiety, and Fuc^a, when present, terminates the sidechain attached to O-6 of Glc^a.

β-D-Glc*p* residues in the backbone. The structures of the eleven oligoglycosyl alditols described in this paper are shown in Fig. 1, along with their coded representation. Note that glucitol residues in oligoglycosyl alditols are represented by the code "Gol".

Specific residues within a xyloglucan oligoglycosyl alditol are designated with superscript lowercase letters. These superscripts reflect the position of each residue vis a vis the D-glucitol moiety. The order of backbone β-D-Glc*p* residues (starting with the nonreducing terminus and progressing toward the β-D-Glc*p* linked to O-4 of the glucitol) is thus $Glc^{c'}$, $Glc^{b'}$, $Glc^{a'}$, Glc^{s}, Glc^{c}, Glc^{b}, and Glc^{a}. That is, Glc^a is the 4,6-linked β-D-Glc*p* moiety linked directly to glucitol and Glc^s is the internal, unbranched 4-linked β-D-Glc*p* residue that is sometimes susceptible to cleavage by EG. Specific sidechain residues are indicated by using the superscript letter of the β-D-Glc*p* residue to which the sidechain is attached. This convention is also illustrated in Fig. 1.

3. Results and discussion

Structures of oligosaccharides released from CW XG and SEPS XG by EG.—Not all of the XG produced by suspension-cultured sycamore cells is incorporated into the cell wall.

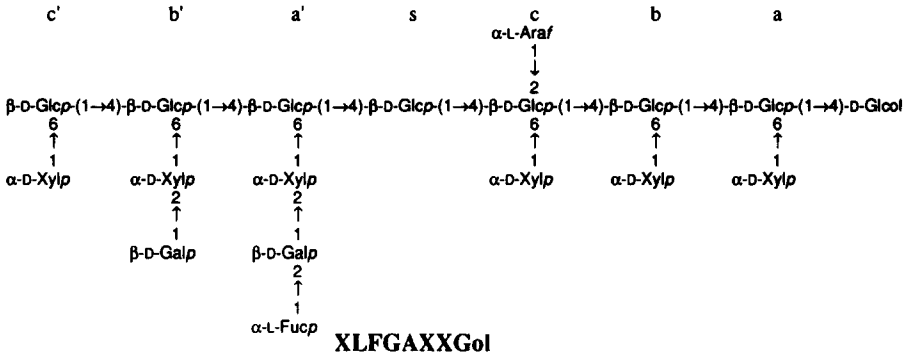

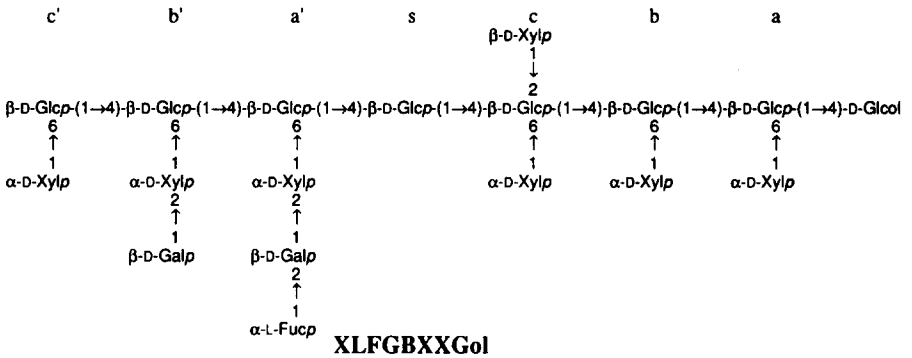

Fig. 1 (continued).

The XG that is secreted into the culture medium is referred to as SEPS XG (i.e., derived from "Sycamore Extracellular PolySaccharides"), and the XG that is incorporated into the Cell Wall is referred to as CW XG. Although the chemical composition of these two forms has been shown to be very similar [5], no thorough comparison of their structures has previously been reported.

Most, if not all, of the α-L-Ara*f* residues and β-D-Xyl*p* residues present in SEPS XG are attached to the backbone via O-2 of β-D-Glc*p* residues [9,19]. Relatively few plant species have been reported to produce XGs with sidechains attached at this position [20], but, when present, they render the adjacent unbranched β-D-Glc*p* residues resistant to EG-catalyzed hydrolysis [9]. The XG oligosaccharides released from purified sycamore cell walls by treatment with EG were isolated and analyzed in parallel with those released from SEPS XG in order to determine whether common structural features lead to EG resistance in SEPS XG and CW XG. Acidic components of the EG-released material were removed by anion-exchange chromatography. The XG oligosaccharides comprising the neutral fraction were separated by size-exclusion chromatography on Bio-Gel P-2. The decasaccharide, nonasaccharide, heptasaccharide, and pentasaccharide fragments, whose structures and presence in SEPS XG and CW XG have been previously described [5,6], were partially included in the P-2 matrix. Relatively high molecular weight fragments (dp > 24) were eluted in the void volume. XG oligosaccharides (dp 17–20) containing an EG-resistant unbranched β-

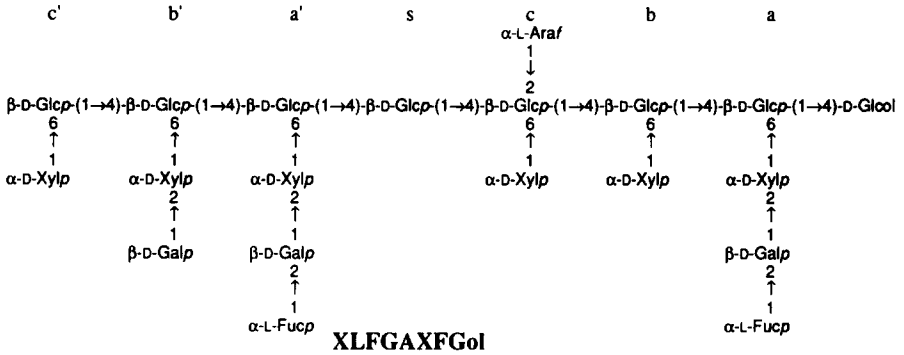

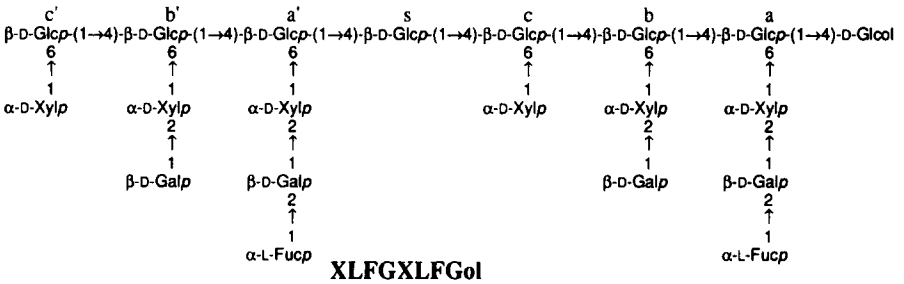

Fig. 1 (continued).

D-Glc*p* residue were eluted as a broad peak (designated P2-2) with $K_{av}=0.11$. (See, for example, Bauer et al. [5] or Hisamatsu et al. [9] for typical P-2 profiles.)

The EG-resistant oligosaccharides (dp 17–20) in fractions SEPS P2-2 and CW P2-2 were further purified by normal-phase HPLC on amino-bonded silica gel (Figs. 2A and 2B). The HPLC eluants were pooled as indicated, affording eight heterogeneous fractions, designated N1–N4 for the SEPS-derived fractions and N5–N8 for the CW-derived fractions. The fractions were each reduced with $NaBH_4$ to yield eight mixtures of oligoglycosyl alditols, designated R1–R4 (SEPS) and R5–R8 (CW). Individual oligoglycosyl alditols were then purified from these mixtures by reversed-phase HLPC on octadecylsilyl silica gel (ODS, Fig 3). We have previously used this approach [9] to purify the oligoglycosyl alditol derivatives of seven EG-resistant SEPS XG oligosaccharides. The SEPS XG oligoglycosyl alditols characterized in that study [9] were found to have the unusual α-L-Ara*f* and/or β-D-Xyl*p* residue-containing sidechains attached to O-2 of backbone β-D-Glc*p* residues. ^{1}H NMR analysis of the oligoglycosyl alditols released from cell walls in the current study clearly showed that all seven of these EG-resistant oligosaccharides (marked with an asterisk {*} in Fig. 4) are also present in CW XG.

In all, eleven previously uncharacterized oligosaccharides were identified in the current study. Six of these, namely, XXBGXXFGol, XXXGBXFGol, XLFGAXXGol, XLFGBXXGol, XLFGAXFGol, and XLFGBXFgol are marked with a check [✓] in Fig. 4. All six oligosaccharides contain unbranched β-(1→4)-linked D-Glc*p* residues that are

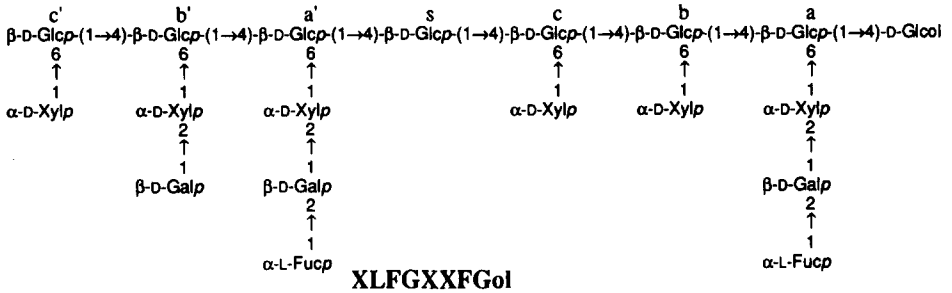

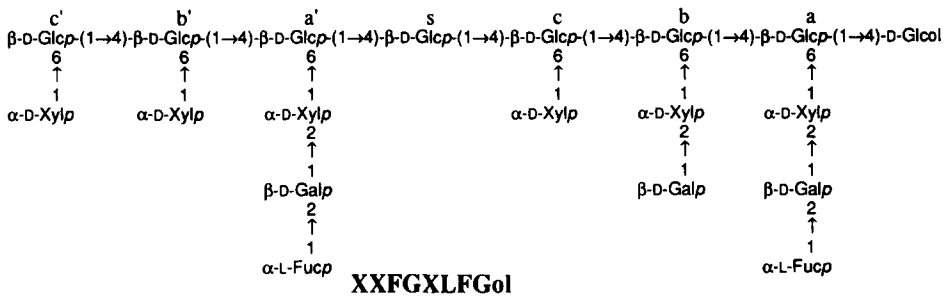

Fig. 1 (continued).

resistant to EG-catalyzed hydrolysis due to the presence of an α-L-Ara*f* or a β-D-Xyl*p* residue at O-2 of one of the two β-D-Glc*p* residues flanking the unbranched β-D-Glc*p* residue. Five other novel oligoglycosyl alditols, namely, XLFGXLFGol, XLFGXXFGol, XXFGXLFGol, XFFGXXFGol, and XXFGXFFGol (marked with a star {☆} in Fig. 4) were purified from the (SEPS) R4 fraction and structurally characterized. These are resistant to EG-catalyzed hydrolysis due to the presence of extended sidechains (i.e., α-L-Fuc*p*-(1→2)-β-D-Gal*p*-(1→2)-α-D-Xyl*p* and/or β-D-Gal*p*-(1→2)-α-D-Xyl*p*) at O-6 of two adjacent β-D-Glc*p* residues somewhere along the backbone. This structural feature has been shown [9] to confer partial EG-resistance to unbranched β-D-Glc*p* residues in the oligosaccharide. Conformational energy calculations suggest that, in this case, the EG-resistance is the result of the folding of extended sidechains onto both surfaces of the ribbon-like backbone [21]. However, the EG-resistance conferred by this structural feature is significantly less pronounced than that of XG oligosaccharides containing a glycosyl substituent at O-2 of one of the β-D-Glc*p* residues flanking the unbranched β-D-Glc*p* residue [9] (see above).

The relative amounts of the various EG-resistant oligosaccharide components in the P2-2 fractions from SEPS XG and CW XG were not identical. Since the presence of two adjacent extended sidechains confers partial EG-resistance to XG oligosaccharides, the relative recovery of these oligosaccharides depends on the amount of EG present in the digestion mixture, the digestion time, and the relative susceptibility of each oligosaccharide to cleavage by the enzyme. In addition, one EG digestion was performed on a soluble substrate (SEPS XG) while the other was performed on an initially insoluble substrate (cell

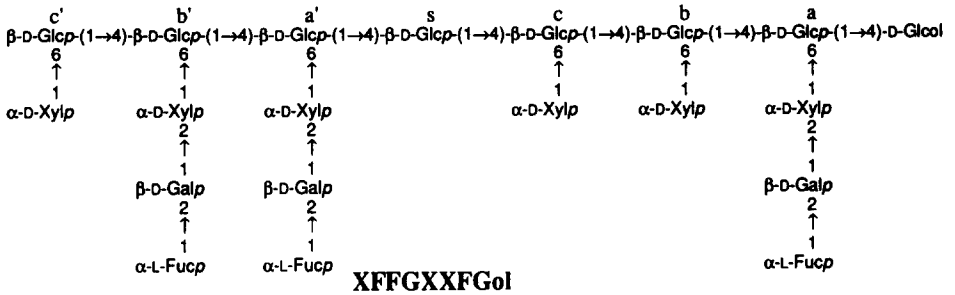

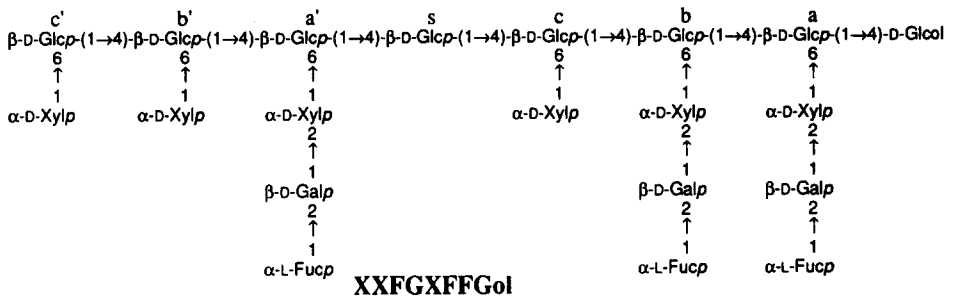

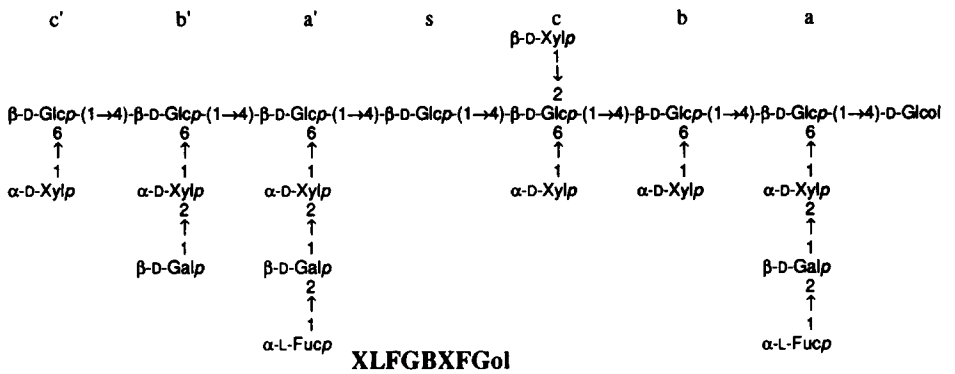

Fig. 1 (continued).

walls), and so the extent of EG-catalyzed hydrolysis of the two samples cannot be directly compared.

The differences in oligosaccharide composition of SEPS P2-2 and CW P2-2 led to differences in their elution profiles on amino-bonded silica gel (Fig. 2), and therefore the pooling of column fractions (based on the location of valleys in the chromatogram) was slightly different for the two samples. Oligosaccharides that eluted at or near one of the valleys in these chromatograms were ultimately detected in different fractions depending

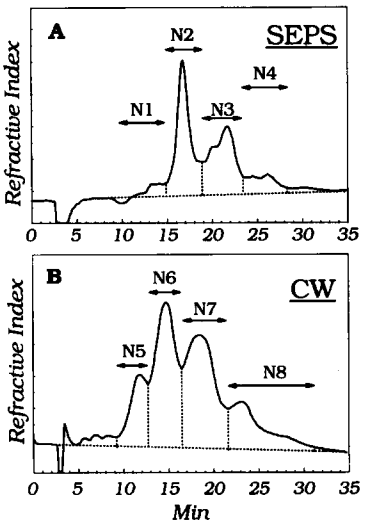

Fig. 2. Normal-phase HPLC on amino-bonded silica gel (Dynamax 60-A). Oligosaccharides with dp 17–20, generated from SEPS XG (Panel A) or cell walls (CW, Panel B), were dissolved (30–40 mg/mL) in water, and 10 μL (Panel A) or 50 μL (Panel B) was injected and eluted with 54% (Panel A) or 62% (Panel B) aqueous MeCN at a flow rate of 1 mL/min. The eluates of several preparative runs (50 μL injected) were pooled as indicated.

on the precise location of the boundary between fractions. Thus, fractions R1–R4, derived from SEPS XG, were significantly different from the analogous fractions R5–R8, derived from CW XG. (See Fig. 4.)

Separation of oligoglycosyl alditols by HPAEC.—Examination of fraction R6-4 by ^{1}H NMR spectroscopy indicated that it contained a mixture of oligoglycosyl alditols. These were resolved by high-pH anion-exchange chromatography (HPAEC) (Fig. 5). One of the three components (R6-4C) isolated from this mixture was XXFGCXXGol, which had been previously characterized [9] after its isolation from SEPS fraction R2-3 by normal-phase chromatography on amino-bonded silica gel. The observation that R6-4 could be separated into three components by HPAE prompted us to reexamine R2-3 (from which XXFGCXXGol had been originally isolated) by HPAE chromatography. The HPAE chromatogram of R2-3 was nearly identical to that of R6-4 (Fig. 5). The first two major components eluted from HPAE column were the isomeric heptadecamers XXBGXXFGol and XXXGBXFGol that differ from each other only in the point of attachment of the β-D-Xyl*p* residue. Previously, the β-D-Xyl*p* residues in XG oligosaccharides had only been found at O-2 of the β-D-Glc*p* residue flanking the unbranched β-D-Glc*p* residue on the side closest to the alditol end (e.g., XXFGBXXGol). However, the β-D-Xyl*p* residue in XXBGXXFGol is in a novel position, i.e., on the nonreducing side of the unbranched β-D-Glc*p* residue. Although XXXG is one of the most common sequences found in sycamore XG, XXXGBXFGol is the only XG oligosaccharide that has been isolated that has an unbranched internal β-D-Glc*p* residue and the structure XXXG at its nonreducing terminus. Thus, the unusual structural features of XXBGXXFGol and XXXGBXFGol make them extremely useful in terms of confirming and extending our list of correlations between the

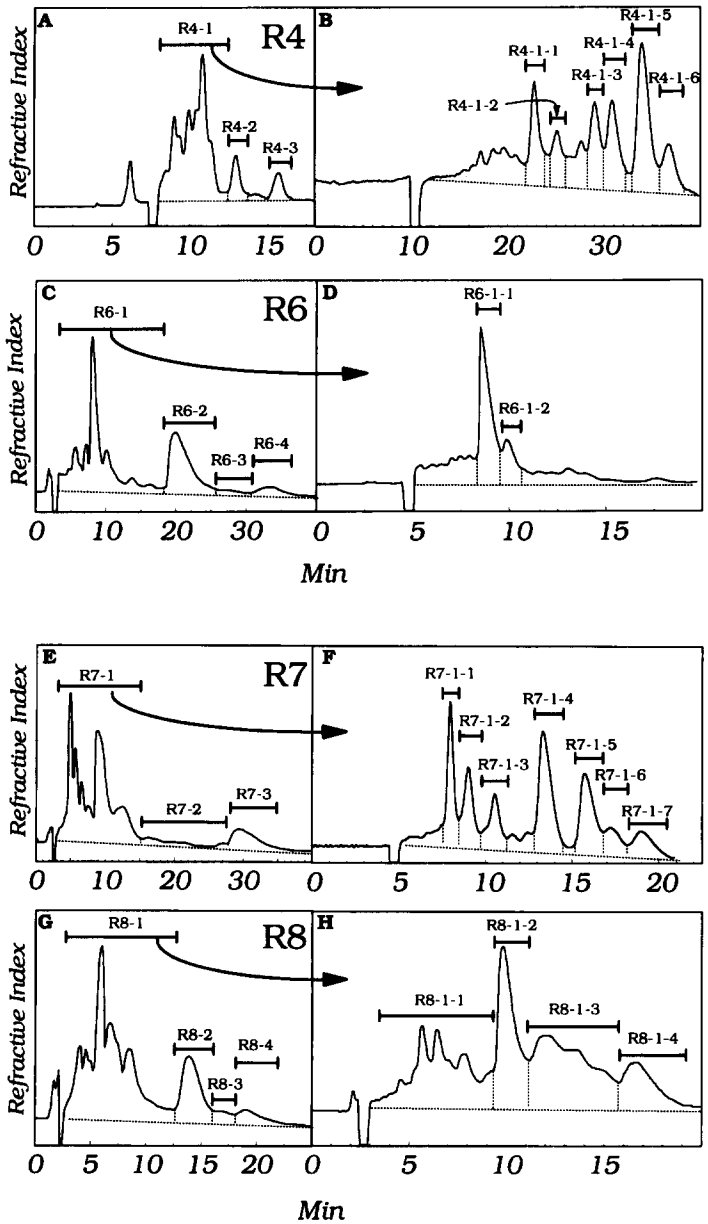

Fig. 3. Reversed-phase HPLC of oligoglycosyl alditols on octadecylsilyl silica gel. The chromatograms of fractions R4, R6, R7, and R8, generated by borohydride reduction of fractions N4, N6, N7, and N8 (Fig. 2), are shown on the left side of the figure (Panels A, C, E, and G, respectively). The early, incompletely separated peaks were pooled as indicated and rechromatographed (Panels B, D, F, and H) under different conditions. Panel A: Fraction R4 (SEPS), 24% MeOH, 2 mL/min, 1.0×25 cm column. Panel B: Fraction R4-1 (SEPS), 21% MeOH, 1.5 mL/min, 1.0×25 cm column. Panel C: Fraction R6 (CW), 18% MeOH, 1 mL/min, 0.25×25 cm column. Panel D: Fraction R6-1 (CW), 21% MeOH, 3 mL/min, 1.0×25 cm column. Panel E: Fraction R7 (CW), 19% MeOH, 1 mL/min, 0.25×25 cm column. Panel F: Fraction R7-1 (CW), 21% MeOH, 3 mL/min, 1.0×25 cm column. Panel G: Fraction R8 (CW), 20% MeOH, 1 mL/min, 0.25×25 cm column. Panel H: Fraction R8-1 (CW). 17.5% MeOH, 1 mL/min, 0.25×25 cm column. Reversed-phase chromatography of R2 and R3, derived from SEPS XG (not shown), are described in [7].

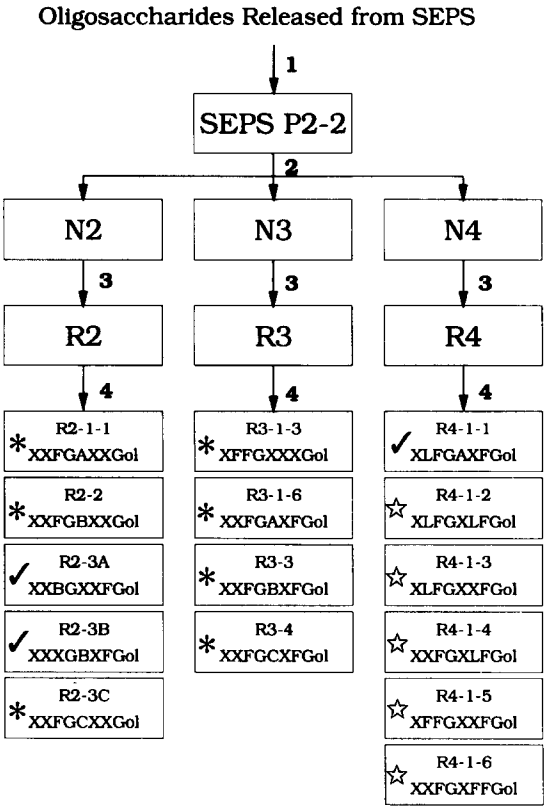

Fig. 4. Schematic summary of the purification of the XG oligoglycosyl alditols. The various fractions are indicated by the text within boxes, and steps involved in their purification are indicated by the numerals outside the boxes. The preparative steps included (1) Bio-Gel P-2 chromatography, (2) normal-phase HPLC, (3) reduction with $NaBH_4$, and (4) reversed-phase HPLC. Fractions whose names end with A, B, or C (e.g., R2-3A) were obtained by HPAEC of the respective reversed-phase fraction. The structure of the dominant oligoglycosyl alditol in each fraction is represented by the shorthand nomenclature described in the text and Table 1. See the text for the significance of the asterisks (*), checks (✓), and stars (☆).

locations and identities of XG sidechains and specific NMR chemical-shift effects (see below).

Determination of oligoglycosyl alditol structures.—The following general approach was used to determine the structures of the purified oligoglycosyl alditols. ^{1}H NMR spectra of the oligoglycosyl alditols were recorded, including two-dimensional COSY and TOCSY spectra when enough material was available. The identities and locations of sidechains of the oligoglycosyl alditols were initially assigned by applying previously reported [6,9,19] correlations between these structural features and specific chemical-shift effects evident in their ^{1}H NMR spectra. In most cases this provided all of the information required to derive the glycosyl sequence. However, the structures of some of the novel oligoglycosyl alditols could not be unambiguously assigned solely on this basis. For example, the locations of the sidechains terminated with a β-D-Gal*p* residue in the isomeric nonadecamers XLFGXXFGol and XXFGXLFGol could not be assigned without knowledge of structure/

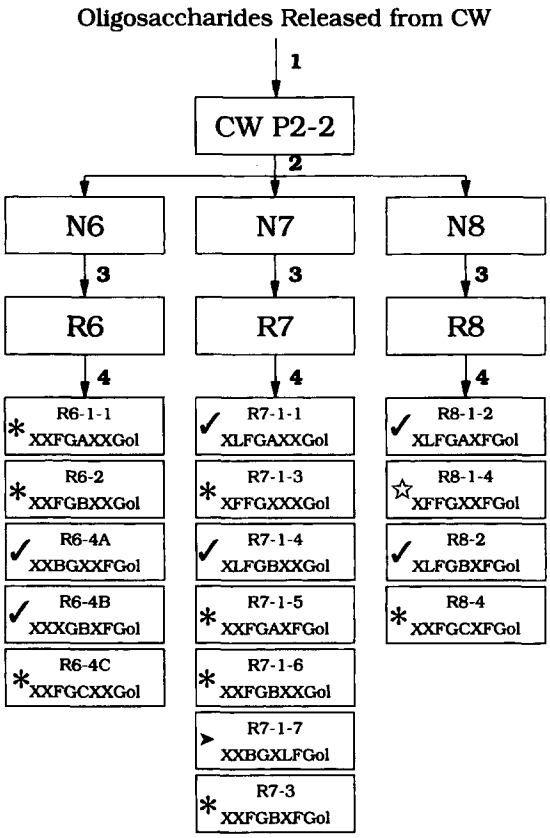

Fig. 4 (continued).

chemical-shift correlations that had not yet been deduced. Therefore, the molecular weights and glycosyl sequences of all of the oligoglycosyl alditols were determined by a combination of mass spectral techniques. The resulting sequence information allowed us to confirm our previously reported structure/chemical-shift correlations and provided a basis upon which additional correlations could be deduced by analysis of the extended set of ^{1}H NMR spectra.

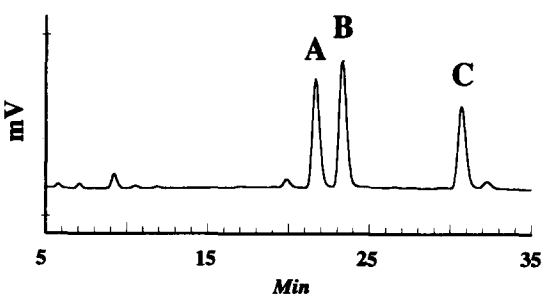

Fig. 5. HPAEC of fraction R6-4, derived from CW XG, on a Dionex CarboPac PA1 column (4×250 mm) eluted with a linear gradient from 60 to 150 mM NaOAc in 100 mM NaOH. The elution profile of fraction R2-3, derived from SEPS XG (data not shown), was nearly indistinguishable from that of R6-4.

Table 2
MALD-TOF mass spectrometry of XG oligoglycosyl alditols

Structure [a]	Fraction	Measured mass [b]	Calculated mass [c]	Composition [d]
XLFGAXFGol [e]	R4-1-1	3042.7	3043.7	$Fuc_2Gal_3AraXyl_6Glc_7Glcol$
XLFGXLFGol	R4-1-2	3072.0	3073.7	$Fuc_2Gal_4Xyl_6Glc_7Glcol$
XLFGXXFGol	R4-1-3	2911.3	2911.6	$Fuc_2Gal_3Xyl_6Glc_7Glcol$
XXFGXLFGol	R4-1-4	2909.7	2911.6	$Fuc_2Gal_3Xyl_6Glc_7Glcol$
XFFGXXFGol	R4-1-5	3058.9	3057.7	$Fuc_3Gal_3Xyl_6Glc_7Glcol$
XXFGXFFGol	R4-1-6	3055.6	3057.7	$Fuc_3Gal_3Xyl_6Glc_7Glcol$
XXBGXXFGol	R6-4A	2574.8	2573.3	$FucGalXyl_7Glc_7Glcol$
XXXGBXFGol	R6-4B	2574.7	2573.3	$FucGalXyl_7Glc_7Glcol$
XLFGAXXGol	R7-1-1	2735.2	2735.4	$FucGal_2AraXyl_6Glc_7Glcol$
XLFGBXXGol	R7-1-4	2735.2	2735.4	$FucGal_2Xyl_7Glc_7Glcol$
XLFGAXFGol [e]	R8-1-2	3041.1	3043.7	$Fuc_2Gal_3AraXyl_6Glc_7Glcol$
XLFGBXFGol	R8-2	3044.4	3043.7	$Fuc_2Gal_3Xyl_7Glc_7Glcol$

[a] See Fig. 1.
[b] All listed ions assigned as $[M+Na]^+$. Accuracy of measurement $\pm 0.1\%$.
[c] Theoretical chemical masses of $[M+Na]^+$ ions calculated by the CARBOMASS program [12].
[d] Composition based on molecular mass and other spectroscopic data.
[e] Fractions R4-1-1 and R8-1-2 both contain XLFGAXFGol as the predominant component.

Determination of molecular weight by MALD-TOF mass spectrometry.—The molecular weights of the newly characterized oligoglycosyl alditols were established by MALD-TOF mass spectrometry (Table 2 and Fig. 6). This technique produced spectra with much greater signal to noise than FABMS (described below) thereby allowing the molecular weights of contaminants in these fractions to be measured.

FABMS analysis of oligoglycosyl alditols.—FABMS analysis of native and *O*-peracetylated derivatives of xyloglucan oligoglycosyl alditols is a powerful technique for deter-

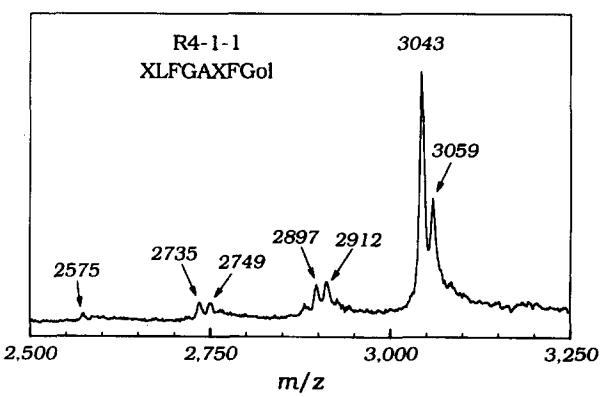

Fig. 6. MALD-TOF spectrum of fraction R4-1-1. Measured ion masses, rounded to the nearest integer, are indicated, and correspond to the chemical mass of the ion $\pm 0.1\%$ (see Table 2). The signals at m/z 3043 and 3059 are due to $[M+Na]^+$ and $[M+K]^+$ pseudomolecular ions, respectively, of the main component, XLFGAXFGol. Other signals are due to impurities that may give rise to the unexpected B_9^+ ion in the positive-ion FAB mass spectrum of the material prepared by *O*-peracetylation of this fraction (see text).

mining the glycosyl sequences of these molecules [9]. Negative-ion FAB mass spectra of underivatized xyloglucan oligoglycosyl alditols are dominated by the pseudomolecular $[M-H]^-$ ion and Y_n^- alditol end fragment ions [22] that arise via cleavage between the glycosidic carbon and glycosidic oxygen. Thus, negative-ion FABMS confirms the glycosyl composition of the oligoglycosyl alditol and establishes the order of sidechain substitution for backbone residues near the alditol. For example, the Y_3^- ion at m/z 475 (XylGlcGlcol) and the Y_5^- ion at m/z 769 (Xyl_2Glc_2Glcol) in the negative-ion FAB-mass spectrum of the oligoglycosyl alditol in R7-1-1 (XLFGAXXGol) confirm that the structure α-D-Xyl*p*-(1→6)-β-D-Glc*p*-(1→4)-[α-D-Xyl*p*-(1→6)]-β-D-Glc*p*-(1→4)-β-D-Glcol is present at the alditol end of the molecule. The location of the α-L-Ara*f* residue in this oligoglycosyl alditol was established by the Y_8^- ion at m/z 1195 ($AraXyl_3Glc_3Glcol$). The presence of a high-abundance Y_5^- ion at m/z 783 (FucGalXylGlcGlcol) in the negative-ion FAB mass spectrum of the oligoglycosyl alditol indicates that an α-L-Fuc*p*-(1→2)-β-D-Gal*p*-(1→2)-α-D-Xyl*p* sidechain is attached to O-6 of the β-D-Glc*p* residue directly linked to the Glcol moiety, as in XXXGBXFGol (fraction R6-4B).

Positive-ion FAB mass spectra of the *O*-peracetylated derivatives of oligoglycosyl alditols are dominated by the $[M+NH_4]^+$ pseudomolecular ion and nonreducing end B_n^+ fragment ions [22] that also arise via cleavage of the bond between the glycosidic carbon and glycosidic oxygen. Thus, positive-ion FABMS analysis confirms the glycosyl composition and provides glycosyl sequence information for the region near the nonreducing termini of these branched molecules. This information complements that obtained by negative-ion FABMS of the underivatized molecules. For example, a sequence of ions B_1^+ at m/z 273 (Fuc), B_2^+ at m/z 561 (FucGal), and B_3^+ at m/z 777 (FucGalXyl) confirms the presence of an α-L-Fuc*p*-(1→2)-β-D-Gal*p*-(1→2)-α-D-Xyl*p* sidechain in the molecule. Usually, one of the most prominent features of these spectra is the very abundant B_n^+ fragment ion formed by cleavage of the bond between C-1 and O-1 of the unbranched β-D-Glc*p* residue in the backbone (i.e., cleavage of the Glc^s–Glc^c glycosidic bond). For example, the presence of α-D-Xyl*p*-(1→6)-β-D-Glc*p*-(1→4)-[α-D-Xyl*p*-(1→6)]-β-D-Glc*p*-(1→4)-[α-L-Fuc*p*-(1→2)-β-D-Gal*p*-(1→2)-α-D-Xyl*p*-(1→6)]-β-D-Glc*p*-(1→4)-β-D-Glc*p* at the nonreducing terminus of XXFGXFFGol (R4-1-6) was established by the strong B_9^+ ion at m/z 2361 (i.e., $FucGalXyl_3Glc_4$), the B_2^+ ion at m/z 547 (i.e., XylGlc), the B_4^+ ion at m/z 1051 (i.e., Xyl_2Glc_2), and the ions (described above) at m/z 273, 561, and 777.

Although the Glc^s–Glc^c glycosidic bond in *O*-peracetylated xyloglucan oligoglycosyl alditols is especially labile during positive-ion FABMS analysis, the $Glc^{a'}$–Glc^s glycosidic bond appears to be especially stable. For example, the spectrum of XXFGXFFGol contains a high-abundance B_9^+ ion at m/z 2361 ($FucGalXyl_3Glc_4$), but the B_8^+ ion at m/z 2073 ($FucGalXyl_3Glc_3$) is barely visible above the chemical noise. The mechanistic basis for this phenomenon is not known.

The positive-ion FAB mass spectra of several of the *O*-peracetylated oligoglycosyl alditols contained higher than expected abundances of the B_n^+ ions corresponding in mass to the unfavored fragmentation described above. Specifically, the B_9^+ ion at m/z 2361 [$DeoxyhexPent_3Hex_5$] was more abundant than expected in the spectra of the *O*-peracetylated derivatives of XLFGAXFGol (R4-1-1 and R8-1-2), XLFGXLFGol (R4-1-2), and XLFGXXFGol (R4-1-3). MALD-TOF (Fig. 6) and ^1H NMR analysis of these fractions indicated that they were contaminated with small amounts (10–20%) of other oligoglycosyl

alditols that could give rise to the B_9^+ ions at m/z 2361 via the favored fragmentation between Glc^s and Glc^c. However, it cannot be ruled out that the presence of a disaccharide sidechain [β-D-Gal*p*-(1→2)-α-D-Xyl*p*] at O-6 of Glc$^{b'}$ in all of these oligoglycosyl alditols somehow increases the likelihood that the normally unfavorable fragmentation between Glc$^{a'}$ and Glc^s will occur, leading to high-abundance B_9^+ ions at m/z 2361 ($FucGal_2 \times yl_3Glc_3$).

Correlations between chemical shifts of ^{1}H NMR signals and specific structural features of the xyloglucan oligoglycosyl alditols.—Generally, the chemical shift of an anomeric proton in a sidechain of a xyloglucan oligoglycosyl alditol is significantly affected by only three structural features: (1) the identity of the glycosyl residue and the structure of the sidechain in which it resides; (2) end effects arising from the location of the sidechain vis a vis the nonreducing or alditol end of the molecule; (3) the presence of other sidechain structures in the immediate vicinity. Specific correlations between these structural features of the oligoglycosyl alditols and the chemical shifts and homonuclear coupling constants of their anomeric (and other diagnostic) protons have been deduced [6,9,19]. These correlations were confirmed, and additional correlations diagnostic for the locations of specific sidechains were deduced by examination of the ^{1}H NMR spectra of the eleven new oligoglycosyl alditols whose structures are reported here.

Diagnostic regions in the ^{1}H NMR spectra of xyloglucan oligoglycosyl alditols.—The ^{1}H NMR spectra of the xyloglucan oligoglycosyl alditols are divided into specific regions labeled with Roman numerals in Fig. 7. The presence of a multiplet (with a specific scalar-coupling pattern) in a specific region is diagnostic for the presence of a specific sidechain in the oligoglycosyl alditol. Furthermore, the precise chemical shift of the resonance within the region is correlated to the location of that sidechain and with the identity and location of other, nearby sidechains. Therefore, each spectral region is divided into several subregions designated by an uppercase letter. For example, region III is divided into subregions III-A, III-B, and III-C (Fig. 7). The α-anomeric protons of large xyloglucan oligoglycosyl alditols are generally well resolved and can be specifically assigned in one-dimensional ^{1}H NMR spectra on the basis of these correlations. The resonances of β-anomeric protons and most of the ring protons in large xyloglucan oligoglycosyl alditols are highly overlapped, and therefore cannot be individually assigned without the aid of multidimensional NMR experiments. Nevertheless, because structural differences between these oligoglycosyl alditols invariably take the form of differences in the number, identity, and location of sidechains rich in α-linked glycosyl residues, it is frequently possible to assign the entire structure of a xyloglucan oligoglycosyl alditol by considering only the α-anomeric proton resonances. Therefore, special attention will be given to the description of spectral regions (I–IV) containing α-anomeric proton resonances, which are summarized in Fig. 7 and Tables 3 and 4. A more complete description of the other diagnostic spectral regions (V–IX), which contain the anomeric resonances of all of the β-linked glycosyl residues, as well as H-2 and H-4 of the α-Ara*f* residues and H-5 and H-6 of the α-Fuc*p* residues, can be found in refs. [6], [9], and [19].

The structure of a XG oligoglycosyl alditol can usually be deduced by comparing the measured chemical shifts of α-anomeric resonances to those listed in Tables 3 and 4. Each column in Tables 3 and 4 refers to a specific substructure (i.e., sidechain substitution pattern), as indicated in the top line of the header, using the shorthand nomenclature

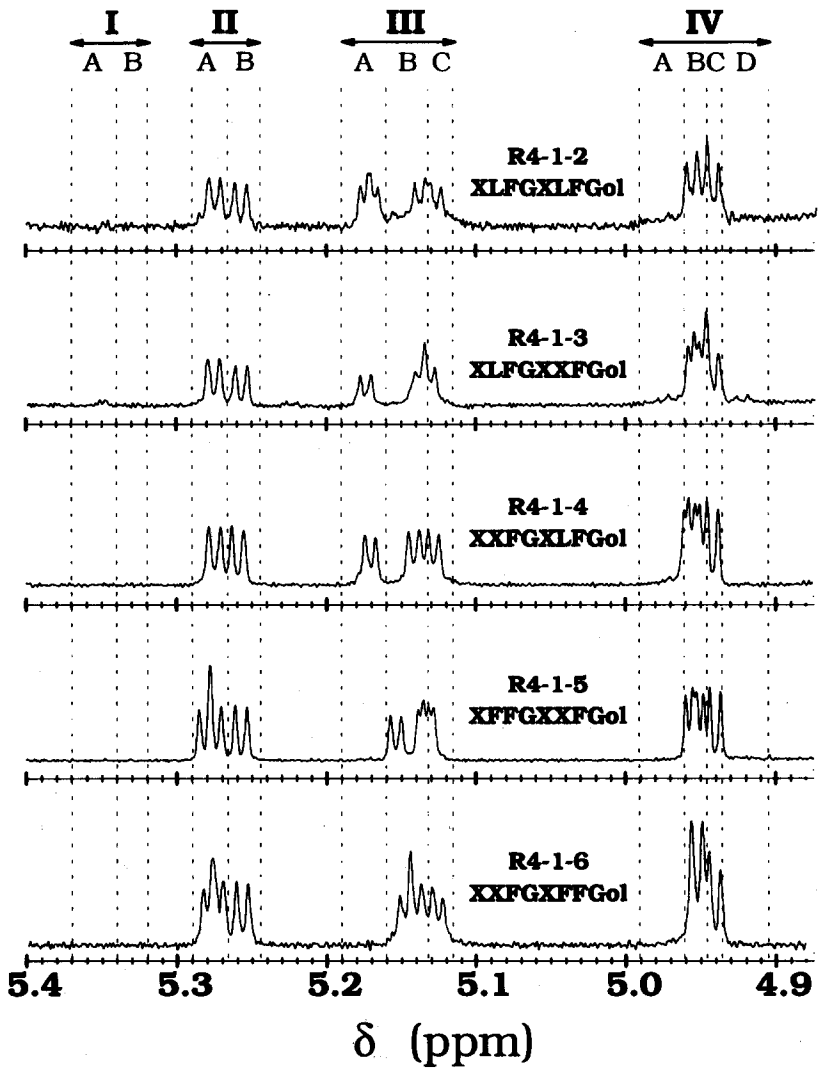

Fig. 7. Partial ^{1}H NMR spectra of the eleven new oligoglycosyl alditols. Regions marked I–IV contain α-anomeric proton signals that are diagnostic for specific substructures in xyloglucan oligoglycosyl alditols (see text and Table 3).

described in Table 1. The lower-case letter in the middle row of the header identifies the position of this substructure in the oligoglycosyl alditol, as defined in Fig. 1. (See also *Nomenclature for XG oligoglycosyl alditols* in the Materials and Methods section.) The bottom row of the header identifies a specific proton resonance that is diagnostic for locating the substructure in the molecule. For example, the first row of Table 3 gives chemical shift values for XLXGol. The XLXGol resonance (H-1 Xyl^b) at δ 5.174 is assigned to the anomeric proton of the α-D-Xyl*p* residue at position "b" (i.e., attached to Glc^b, the middle β-D-Glc*p* residue in this molecule). The chemical shift of this resonance is diagnostic for substructure "L" [β-D-Gal*p*-(1→2)-α-D-Xyl*p*-(1→6)-β-D-Glc*p*] at position "b".

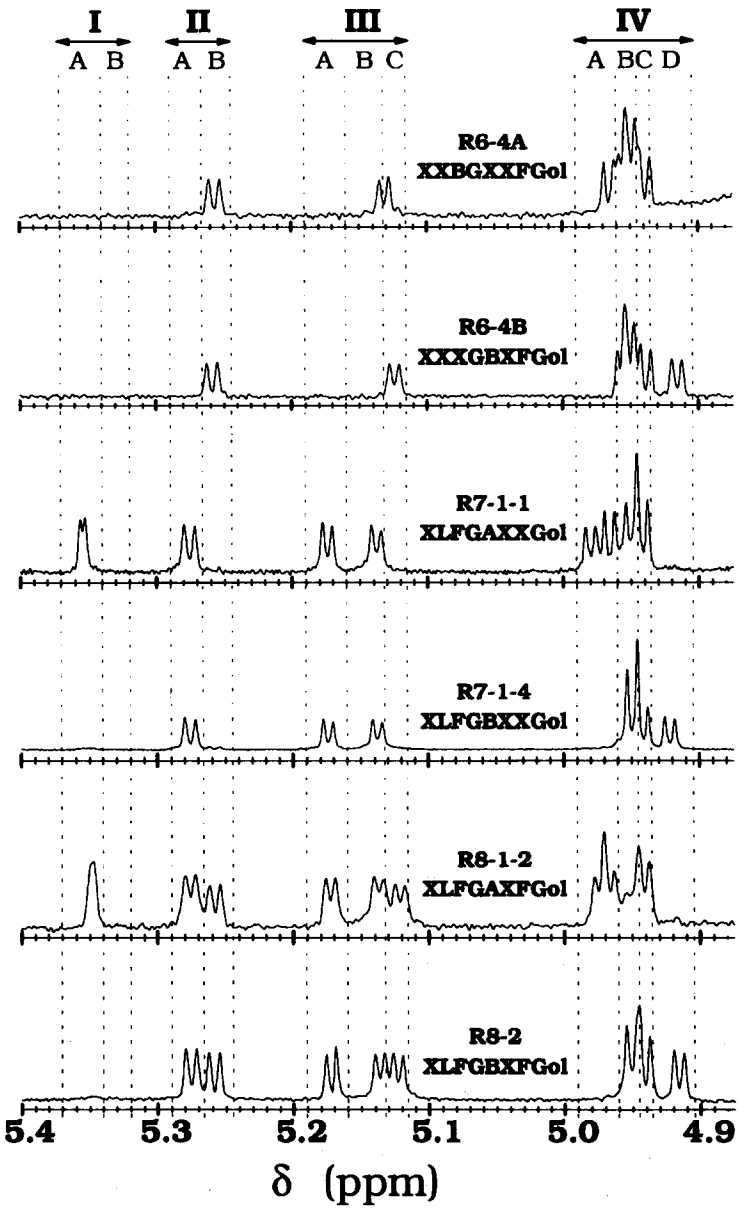

Fig. 7 (continued).

Small chemical shift variations in each column provide information on the identity and location of other sidechains in the oligoglycosyl alditol, as described below.

Region I (δ 5.37–5.32) contains the H-1 resonances ($^3J_{1,2} \approx 2$ Hz) of α-L-Ara*f* residues in sidechains attached to O-2 of β-D-Glc*p* residues in the backbone. If the sidechain consists of a single terminal α-L-Ara*f* residue, the resonance is in region I-A (δ 5.340–5.370). If the sidechain consists of the α-L-Ara*f*-(1→3)-β-D-Xyl*p*, the resonance is in region I-B (δ

Table 3
Chemical shifts of α-anomeric resonances of XG oligoglycosyl alditols

Substructure [a]	F	F	F	F	F	F	F	F	L	L	L	L
Position [b]	b′	a′	b	a	b′	a′	b	a	b′	a′	b	a
Resonance [c]	H-1	H-1	H-1	H-1	H-1	H-1	H-1	H-1	H-1	H-1	H-1	H-1
	$Fuc^{b'}$	$Fuc^{a'}$	Fuc^{b}	Fuc^{a}	$Xyl^{b'}$	$Xyl^{a'}$	Xyl^{b}	Xyl^{a}	$Xyl^{b'}$	$Xyl^{a'}$	Xyl^{b}	Xyl^{a}
XLXGol											5.174	
XXLGol												5.163
XLLGol											5.173	5.160
XXFGol				5.257				5.131				
XLFGol				5.258				5.126			5.172	
XFFGol			5.279	5.257			5.149	5.126				
XXFGAXXGol		5.274				5.141						
XXFGBXXGol		5.273				5.138						
XXFGCXXGol [d]		5.273				5.140						
XFFGXXXGol	5.281	5.273			5.151 [e]	5.133 [e]						
XXFGAXFGol		5.274		5.258		5.139		5.121				
XXFGBXFGol		5.273		5.258		5.138		5.122				
XXFGCXFGol		5.273		5.258		5.138		5.122				
XLFGAXXGol		5.276				5.138			5.174			
XLFGBXXGol		5.276				5.138			5.174			
XLFGAXFGol		5.276		5.259		5.139		5.122	5.174			
XLFGXLFGol		5.275		5.258		5.138		5.127	5.175		5.170	
XLFGXXFGol		5.275		5.256		5.137		5.131	5.173			
XXFGXLFGol		5.274		5.258		5.140		5.127			5.170	
XFFGXXFGol	5.281	5.274		5.257	5.153	5.134		5.131				
XXFGXFFGol		5.272	5.279	5.256		5.140	5.147	5.125				
XXBGXXFGol				5.256				5.131				
XXXGBXFGol				5.258				5.124				
XLFGBXFGol		5.275		5.258		5.137		5.123	5.172			

[a] A substructure consists of a backbone β-D-Glc*p* residue and its pendant sidechains, as defined in Table 1 and [15].

[b] The position of the substructure in the molecule, as defined in Materials and Methods and Fig. 1.

[c] The resonance diagnostic for locating the substructure indicated in the top row at the position indicated in the middle row.

[d] The chemical shifts originally published for XXFGCXXGol [7] were obtained at 296 K, but all those listed here were obtained at 300 K.

[e] These two resonances were assigned incorrectly in [7].

5.320–5.340). Both of the newly described oligoglycosyl alditols, XLFGAXXGol and XLFGAXFGol, contain an α-L-Ara*f* residue attached directly to the backbone, and their diagnostic resonances are in region I-A. (Oligoglycosyl alditols containing α-L-Ara*f* residues whose H-1 signals are in region I-B are described in [9].) The oligoglycosyl alditols derived from the xyloglucans of Solanaceous plants also have α-L-Ara*f* residues, but these are linked to O-2 of α-D-Xyl*p* residues (as opposed to O-3 of β-D-Xyl*p* residues or O-2 of β-D-Glc*p* residues). Thus, the H-1 resonances of the α-L-Ara*f* residues in the *Solanaceae* XGs have distinctly different chemical shifts and are found in region III (see below).

Region II (δ 5.245–5.290) contains the H-1 resonances ($^3J_{1,2} \approx 4$ Hz) of α-L-Fuc*p* residues that are invariably found at the terminus of α-L-Fuc*p*-(1→2)-β-D-Gal*p*-(1→2)-α-D-Xyl*p* sidechains attached to O-6 of a backbone β-D-Glc*p* residue. When the α-L-Fuc*p* residue terminates a sidechain attached to Glc^a (next to the alditol), its H-1 resonance is

Table 4
Chemical shifts of α-anomeric resonances of XG oligoglycosyl alditols

Substructure [a]	X	X	A	A	A	B	B	C	C
Position [b]	c′	c	c	c	c	a′	c	c	c
Resonance [c]	H-1 Xyl$^{c'}$	H-1 Xyl^{c}	H-1 Xyl^{c}	H-1 Xyl^{b}	H-1 Ara^{c}	H-1 Xyl$^{b'}$	H-1 Xyl^{b}	H-1 Xyl^{b}	H-1 Ara^{c}
XLXGol		4.940							
XXLGol		4.938							
XLLGol		4.941							
XXFGol		4.941							
XLFGol		4.941							
XFFGol		4.939							
XXFGAXXGol	4.940		4.966	4.980	5.354				
XXFGBXXGol	4.939						4.921		
XXFGCXXGol [d]	4.941							4.924	5.333
XFFGXXXGol	4.939								
XXFGAXFGol	4.939		4.966	4.974	5.348				
XXFGBXFGol	4.939						4.915		
XXFGCXFGol	4.939							4.917	5.332
XLFGAXXGol	4.942		4.966	4.980	5.354				
XLFGBXXGol	4.942						4.922		
XLFGAXFGol	4.942		4.968	4.976	5.349				
XLFGXLFGol	4.942								
XLFGXXFGol	4.941								
XXFGXLFGol	4.941								
XFFGXXFGol	4.939								
XXFGXFFGol	4.940								
XXBGXXFGol	4.939					4.965			
XXXGBXFGol	4.939						4.916		
XLFGBXFGol	4.941						4.916		

[a] A substructure consists of a backbone β-D-Glc*p* residue and its pendant sidechains, as defined in Table 1 and [15].
[b] The position of the substructure in the molecule, as defined in Materials and Methods and Fig. 1.
[c] The resonance diagnostic for locating the substructure indicated in the top row at the position indicated in the middle row.
[d] The chemical shifts originally published for XXFGCXXGol [7] were obtained at 296 K, but all those listed here were obtained at 300 K.

found in region II-B (δ 5.257 ± 0.001). All other α-L-Fuc*p* H-1 resonances are in region II-A. When an α-L-Fuc*p* residue terminates a sidechain located between a sidechain consisting of a single terminal α-D-Xyl*p* residue and another α-L-Fuc*p*-(1→2)-β-D-Gal*p*-(1→2)-α-D-Xyl*p* sidechain, as in XFFGol, XFFGXXXGol, and XXFGXAFGol, its H-1 signal (in region II-A) is slightly downfield (δ 5.280 ± 0.001) compared to the H-1 signal (δ 5.274 ± 0.002) of an α-L-Fuc*p* residue that terminates a sidechain attached to Glc$^{a'}$ (i.e., next to the unbranched β-D-Glc*p* residue), as in XXFGAXXGol and XFFGXXFGol. Other signals diagnostic for the position of α-L-Fuc*p*-(1→2)-β-D-Gal*p*-(1→2)-α-D-Xyl*p* sidechains are found in region III.

Region III (δ 5.115–5.190) contains H-1 resonances of α-D-Xyl*p* residues with a β-D-Gal*p* residue at O-2 as well as H-1 resonances of α-L-Ara*f* residues in the α-L-Ara*f*-(1→2)-α-D-Xyl*p* sidechains characteristic of the xyloglucans produced by the *Solanacea*. These

two types of anomeric resonances can be easily distinguished by their coupling constants ($^3J_{1,2} \approx 4$ Hz for α-D-Xyl*p*, $^3J_{1,2} < 2$ Hz for α-L-Ara*f*). The α-L-Ara*f* anomeric resonances in region III will not be discussed further, as the XG oligoglycosyl alditols described in this paper do not contain α-L-Ara*f*-(1→2)-α-D-Xyl*p* sidechains.

Region III-A (δ 5.160–5.190) contains the anomeric proton resonances of those α-D-Xyl*p* residues that have a *terminal* β-D-Gal*p* substituent at O-2. When the β-D-Gal*p*-(1→2)-α-D-Xyl*p* sidechain is attached at O-6 of Glc^a as in XXLGol and XLLGol, the H-1 resonance of the 2-linked α-D-Xyl*p* residue is shifted upfield ($\delta 5.161 \pm 0.002$) relative to the analogous resonance when the sidechain is on a different β-D-Glc*p* residue. This resonance is at lowest field ($\delta 5.173 \pm 0.001$) when the sidechain is attached to the penultimate β-D-Glc*p* residue as in XLFGol, XLXGol, and XLFGXXFGol. The H-1 resonances of the α-D-Xyl*p* residues in the β-D-Gal*p*-(1→2)-α-D-Xyl*p* sidechains of XXFGXLFGol and XLFGXLFGol are observed at δ 5.170.

The anomeric proton resonances of α-D-Xyl*p* residues that have an α-L-Fuc*p*-(1→2)-β-D-Gal*p* moiety at O-2 are found in regions III-B and III-C. When a sidechain with this structure is attached to Glc^a, as in XXFGol, XXBGXXFGol, and XXXGBXFGol, the anomeric proton resonance of the 2-linked α-D-Xyl*p* residue is in region III-C (δ 5.115–5.133). The exact chemical shift of this resonance is significantly affected by the presence of β-D-Gal*p* and α-L-Fuc*p*-(1→2)-β-D-Gal*p* moieties that sometimes extend the adjacent sidechain (on Glc^b) and by substituents at O-2 of Glc^c. Both of these structural motifs shift the H-1 resonance of the 2-linked Xyl^a residue to the upfield portion of region III-C. (Compare, for example, XXFGol [Xyl^a H-1 at δ 5.131] to XLFGol [Xyl^a H-1 at δ 5.126] and XXBGXXFGol [Xyl^a H-1 at δ 5.131] to XXXGBXFGol [Xyl^a H-1 at δ 5.124].) The results of computer modeling of the xyloglucan oligosaccharides are consistent with these observations in that they indicate that fucose-containing sidechains on Glc^a have significant interactions with sidechains on Glc^b. Substituents on O-2 of Glc^c also interact with the sidechain on Glc^b (see below), and may thus have an *indirect* effect on the chemical shift of the α-anomeric proton of Xyl^a (via the sidechain on Glc^b). The indirect effect of the O-2 substituents of Glc^c upon the chemical shift of the α-anomeric proton of the 2-linked Xyl^a residue is the only significant "long-range" interaction thus far observed in the ^{1}H NMR spectra of xyloglucan oligoglycosyl alditols; all other observed interactions are between sidechains on adjacent β-D-Glc*p* residues.

When an α-L-Fuc*p*-(1→2)-β-D-Gal*p*-(1→2)-α-D-Xyl*p* sidechain is attached to any β-D-Glc*p* residue *except* Glc^a (next to the alditol), the anomeric proton resonance of the 2-linked α-D-Xyl*p* residue in the sidechain is found in region III-B (δ 5.133–5.160). The α-D-Xyl*p* H-1 resonance has a chemical shift of 5.150 ± 0.003 when this sidechain is between a sidechain consisting of a terminal α-D-Xyl*p* residue and another fucose-containing sidechain, as in XFFGol and XXFGXFFGol. The α-D-Xyl*p* H-1 resonance is found at $\delta\ 5.139 \pm 0.002$ when the fucose-containing sidechain is between a terminal α-D-Xyl*p* sidechain and an unbranched β-D-Glc*p* residue (as in XXFGAXXGol), or between a β-D-Gal*p*-(1→2)-α-D-Xyl*p* sidechain and an unbranched β-D-Glc*p* residue (as in XLFGAXXGol). The α-D-Xyl*p* H-1 resonance is found at $\delta\ 5.133 \pm 0.001$ when the fucose-containing sidechain is between another α-L-Fuc*p*-(1→2)-β-D-Gal*p*-(1→2)-α-D-Xyl*p* sidechain and an unbranched β-D-Glc*p* residue (as in XFFGXXXGol).

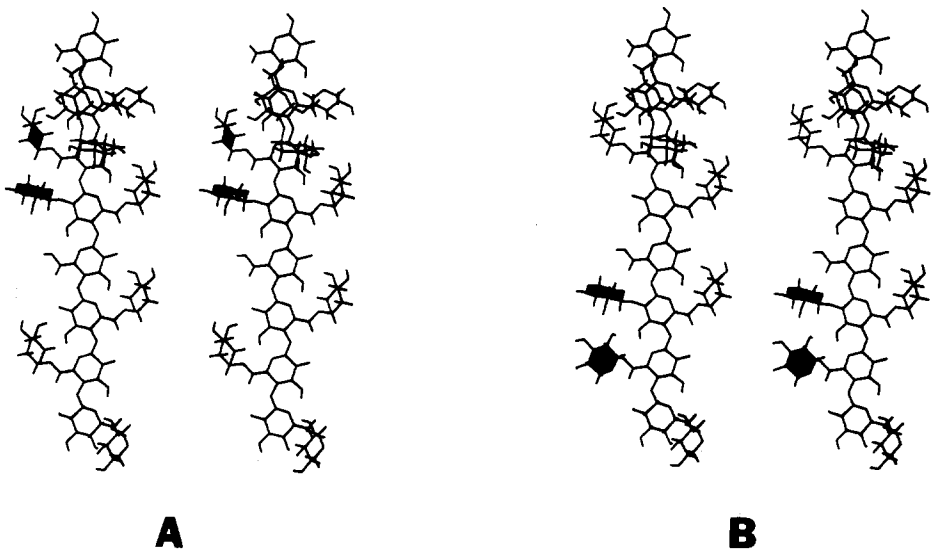

Fig. 8. Relaxed stereoviews of energetically accessible conformations of two closely related oligosaccharides, XXXGBXFG (Panel A) and XXBGXXFG (Panel B) showing the interaction (shaded residues) of β-D-Xyl*p* and α-D-Xyl*p* sidechains. The reducing ends of the oligosaccharides are at the top.

Region IV (δ 4.905–4.990) contains the anomeric proton resonances of terminal α-D-Xyl*p* residues. Unless affected by proximity to the nonreducing end of the backbone or the presence of substituents on O-2 of an adjacent β-D-Glc*p* residue, the anomeric proton resonance of a terminal α-D-Xyl*p* residue is generally found in region IV-B (δ 4.945–4.960), as in XXXGol, XLFGXLFGol, and XXFGXFFGol. However, when the α-D-Xyl*p* residue is on the last β-D-Glc*p* residue (at the nonreducing end) of the backbone, its H-1 resonance is found in region IV-C (δ 4.935–4.945), as in XXXGol, XLFGXLFGol, and XXFGXFFGol. All of the oligoglycosyl alditols described here have a terminal α-D-Xyl*p* residue on the β-D-Glc*p* residue at the nonreducing end of the backbone. Treatment of any of these oligoglycosyl alditols with an α-D-xylosidase that selectively hydrolyzes the α-D-Xyl*p* residue in this position [23] results in a product whose ^{1}H NMR spectrum does not contain a signal in region IV-C.

The interaction of a terminal α-Xyl^b residue with a sidechain attached to O-2 of Glc^c shifts the H-1 resonance of the α-Xyl^b residue from region IV-B into region IV-A or IV-D. This provides a means of detecting and discriminating between α-L-Ara*f* and β-D-Xyl*p* residues linked to O-2 of Glc^c. Thus, even though the anomeric proton of a β-D-Xyl*p* residue linked to O-2 of Glc^c (δ 4.72–4.78) is usually obscured by the HDO signal in one-dimensional ^{1}H NMR spectra, the β-D-Xyl*p* residue is revealed by an α-anomeric resonance ($^3J_{1,2} \approx 4$ Hz) in region IV-D (δ 4.905–4.935), as in XXFGBXXGol, XXFGCXXGol, and XXXGBXFGol. The β-D-Xyl*p* at O-2 of Glc^c is in close proximity to the α-D-Xyl*p* substituent at O-6 of Glc^b residue because the preferred backbone conformation of xyloglucan oligomers [21] places substituents at O-2 of a backbone β-D-Glc*p* residue on the same side of the molecule as the substituents at O-6 of the two adjacent β-D-Glc*p* residues (see Fig. 8). The interaction of the β-D-Xyl*p* substituent at O-2 of Glc^c with the terminal α-D-Xyl*p* substituent at O-6 of Glc^b deshields H-1 of this α-D-Xyl*p* residue so that it is observed in

region IV-D (rather than in region IV-B). Only one α-D-Xyl*p* H-1 resonance is affected by the β-D-Xyl*p* sidechain on Glc^c because Glc^s does not have an α-D-Xyl*p* substituent.

The chemical shifts of those α-D-Xyl*p* H-1 resonances that are shifted into region IV-D by a β-D-Xyl*p* residue at C-2 of Glc^c are significantly affected by the structure of the sidechain attached to Glc^a, but are *not* affected by the presence of an α-L-Ara*f* residue at O-3 of the β-D-Xyl*p* residue. Thus, when Glc^a has an α-L-Fuc*p*-(1→2)-β-D-Gal*p*-(1→2)-α-D-Xyl*p* sidechain at O-6, as in XXFGBXFGol and XXFGCXFGol, the α-Xyl^b H-1 resonance in region IV-D is observed at δ 4.916 ± 0.001. Conversely, when the sidechain attached to O-6 of Glc^a does not contain Fuc or Gal residues, as in XXFGBXXGol and XXFGCXXGol, the α-Xyl^b H-1 resonance in region IV-D is observed at δ 4.922 ± 0.002. The observation that the structure of the sidechain on Glc^a has an effect on the chemical shift of the α-anomeric proton resonance in region IV-D is consistent with the specific assignment of this resonance to H-1 of (terminal) α-Xyl^b (and not to H-1 of α-Xyl^c, for example), because the fucose-containing sidechain at O-6 of Glc^a interacts significantly with the sidechain at O-6 of Glc^b. (See the description of region III-C, above.)

One of the newly described oligoglycosyl alditols (XXBGXXFGol) is unusual in that it has a β-D-Xyl*p* substituent at O-2 of Glc$^{a'}$. The α-D-Xyl*p* residue at O-6 of Glc$^{b'}$ is the only sidechain residue that can directly interact with this β-D-Xyl*p* residue (Fig. 8). The directionality of the backbone imposes a geometry on this interaction that is different than that of a β-D-Xyl*p* residue on Glc^c interacting with an α-D-Xyl*p* residue on Glc^b, described above. This difference is reflected in the downfield (rather than upfield) shift of the α-Xyl$^{b'}$ H-1 resonance (δ 4.965) of XXBGXXFGol into region IV-A. Thus, a signal in region IV-A is diagnostic for a β-D-Xyl*p* substituent at O-2 of a β-D-Glc*p* residue only if the next β-D-Glc*p* residue (toward the *nonreducing* end) bears a terminal α-D-Xyl*p* residue at O-6. This correlation should be invoked judiciously because region IV-A also contains H-1 resonances of terminal α-D-Xyl*p* residues deshielded by α-L-Ara*f* substituents at O-2 of Glc^c (see below).

The H-1 resonances of *two* terminal α-D-Xyl*p* residues are shifted into region IV-A when an α-L-Ara*f* residue is present at O-2 of Glc^c. Note that the effect is opposite that observed when a β-D-Xyl*p* residue is present *at this position* (i.e., deshielding rather than shielding of α-Xyl anomeric protons). The H-1 resonances of the terminal α-D-Xyl*p* residues at O-6 of the adjacent Glc^b and at O-6 of the same Glc^c that bears the α-L-Ara*f* substituent at O-2 are both shifted into region IV-A (δ 4.960–4.990). The two signals that are shifted into region IV-A by the α-L-Ara*f* residue at O-2 of Glc^c can be distinguished because the chemical shift of the terminal α-D-Xyl*p* residue at O-6 of Glc^b is sensitive to the structure of the sidechain at O-6 of Glc^a. That is, when Glc^a bears a fucose-containing sidechain, as in XLFGAXFGol, the most downfield resonance in region IV-A is observed at δ 4.975 ± 0.001, but when Glc^a bears a terminal α-D-Xyl*p* sidechain, as in XLFGAXXGol, the most downfield resonance in region IV-A is observed at δ 4.980 ± 0.001. In both cases (XLFGAXFGol and XLFGAXXGol and similar pairs) the most upfield signal in region IV-A is at δ 4.967 ± 0.001. Therefore, the most downfield resonance (δ 4.980 or 4.975) shifted into region IV-A by an α-L-Ara*f* residue at O-2 of Glc^c is assigned as H-1 of the terminal α-D-Xyl*p* residue at O-6 of Glc^b, and the most upfield resonance (δ 4.967) shifted into region IV-A is assigned to H-1 of the terminal α-D-Xyl*p* residue at O-6 of Glc^c.

Analysis of the newly described xyloglucan oligoglycosyl alditols also confirmed the previously described correlations [9] between structural features and resonances in regions V–IX. It is more difficult to obtain structural information by examination of these regions in one-dimensional spectra due to interference by the HDO signal in region V, significant signal overlap in regions VI and VII, and the limited number of resonances in regions VIII and IX. Nevertheless, analysis of these regions confirms the structural assignments made on the basis of resonances in regions I–IV, and thus it is advisable to examine these regions and determine (by signal integration) the number of protons giving rise to resonances in these regions.

4. Conclusions

The identity and location of specific substructures of XG oligoglycosyl alditols are correlated with the chemical shifts of diagnostic resonances in their ^{1}H NMR spectra. These correlations allow the structures of XG oligoglycosyl alditols prepared by the borohydride reduction of the oligosaccharides enzymically released from polymeric xyloglucans to be determined by analysis of their one-dimensional ^{1}H NMR spectra. Confirmatory structural information can be obtained by analysis of their chromatographic properties and diagnostic fragmentation patterns during FABMS analysis. These results should make it feasible to perform detailed studies of the modification of xyloglucans by various enzymes, using oligosaccharide substrates having a backbone consisting of more than four β-D-Glc*p* residues, and thereby lead to a greater understanding of the mechanisms, kinetics, and biological consequences of xyloglucan metabolism in growing plant cell walls.

Acknowledgements

This research is supported by United States Department of Energy (DOE) grant DE-FG05-93ER20115, and by the DOE-funded (DE-FG09-93ER20097) Center for Plant and Microbial Complex Carbohydrates. The authors are indebted to Dennis Warrenfeltz for continuing technical support and maintenance of the NMR and mass spectrometers.

References

[1] T. Hayashi, *Annu. Rev. Plant Physiol. Plant Mol. Biol.*, 40 (1989) 139–168.
[2] S.C. Fry, R.C. Smith, K.F. Renwick, D.J. Martin, S.K. Hodge, and K.J. Matthews, *Biochem J.*, 282 (1992) 821–828.
[3] J. de Silva, C.D. Jarman, D.A. Arrowsmith, M.S. Stronach, S. Chengappa, C. Sidebottom, and J.S.G. Reid, *Plant J.*, 3 (1993) 701–711.
[4] K. Nishitani and R. Tominaga, *J. Biol. Chem.*, 267 (1992) 21058–21064.
[5] W.D. Bauer, K.W. Talmadge, K. Keegstra, and P. Albersheim, *Plant Physiol.*, 51 (1973) 174–187.
[6] W.S. York, H. van Halbeek, A.G. Darvill, and P. Albersheim, *Carbohydr. Res.*, 200 (1990) 9–31.
[7] W.S. York, J.E. Oates, H. van Halbeek, A.G. Darvill, P. Tiller, and A. Dell, *Carbohydr. Res.*, 173 (1988) 113–132.

[8] L.L. Kiefer, W.S. York, A.G. Darvill, and P. Albersheim, *Phytochemistry*, 28 (1989) 2105–2107.
[9] M. Hisamatsu, W.S. York, A.G. Darvill, and P. Albersheim, *Carbohydr. Res.*, 227 (1992) 45–71.
[10] M. Hisamatsu, G. Impallomeni, W.S. York, P. Albersheim, and A.G. Darvill, *Carbohydr. Res.*, 211 (1991) 117–129.
[11] W.S. York, A.G. Darvill, M. McNeil, T.T. Stevenson, and P. Albersheim, *Methods Enzymol.*, 118 (1985) 3–40.
[12] F. Cervone, G. De Lorenzo, L. Degra, and G. Salvi, *Plant Physiol.*, 85 (1987) 626–630.
[13] A. Dell and P.R. Tiller, *Biochem. Biophys. Res. Commun.*, 135 (1985) 1126–1134.
[14] W.S. York, R.S. Doubet, A.G. Darvill, and P. Albersheim, *Int. Carbohydr. Symp., XIVth, Stockholm, Sweden*, 1988, *Abstr.*, A9.
[15] M. Rance, O.W. Sorensen, G. Bodenhausen, G. Wagner, R.R. Ernst, and K. Wuthrich, *Biochem. Biophys. Res. Commun.*, 117 (1983) 479–485.
[16] A. Bax and D.G. Davis, *J. Magn. Reson.*, 65 (1985) 355–360.
[17] R. Stuike-Prill and B. Meyer, *Eur. J. Biochem.*, 194 (1990) 903–919.
[18] S.C. Fry, W.S. York, P. Albersheim, A. Darvill, T. Hayashi, J.-P. Joseleau, Y. Kato, E.P. Lorences, G.A. Maclachlan, M. McNeil, A.J. Mort, J.S.G. Reid, H.U. Seitz, R.R. Selvendran, A.G.J. Voragen, and A.R. White, *Physiol. Plant.*, 89 (1993) 1–3.
[19] L.L. Kiefer, W.S. York, P. Albersheim, and A.G. Darvill, *Carbohydr. Res.*, 197 (1990) 139–158.
[20] W.T. Mabusela, A.M. Stephen, A.L. Rodgers, and D.A. Gerneke, *Carbohydr. Res.*, 203 (1990) 336–340.
[21] S. Levy, W.S. York, R. Stuike-Prill, B. Meyer, and L.A. Staehelin, *Plant J.*, 1 (1991) 195–215.
[22] C.E. Costello and J.E. Vath, *Methods. Enzymol.*, 193 (1990) 738–768.
[23] C. Augur, L. Yu, K. Sakai, T. Ogawa, P. Sinaij, A.G. Darvill, and P. Albersheim, *Plant Physiol.*, 99 (1992) 180–185.